Removal of spin degeneracy in *p*-SiGe quantum wells demonstrated by spin photocurrents

S. D. Ganichev,[1,2] U. Rössler,[1] W. Prettl,[1] E. L. Ivchenko,[2] V. V. Bel'kov,[2] R. Neumann,[3] K. Brunner,[3] and G. Abstreiter[3]

[1]*Fakultät für Physik Universität Regensburg, D-93040 Regensburg, Germany*

[2]*A. F. Ioffe Physico-Technical Institute, Russian Academy of Sciences, 194021 St. Petersburg, Russia*

[3]*Walter Schottky Institute, TU Munich, D-85748 Garching, Germany*

Spin photocurrents requiring a system lacking inversion symmetry, become possible in SiGe based quantum well (QW) structures due to their built-in asymmetry. We report on circular and linear photogalvanic effects induced by infrared radiation in (001)- and (113)-oriented *p*-Si/Si$_{1-x}$Ge$_x$ QW structures and analyze the observations in view of the possible symmetry of these structures. The circular photogalvanic effect arises due to optical spin orientation of free carriers in QW's with spin-split subbands. It results in a directed motion of free carriers in the plane of the QW. We discuss possible microscopic mechanisms that could remove the spin degeneracy of the electronic subband states.

I. INTRODUCTION

The spin degrees of freedom of charge carriers and its manipulation has become a topical issue in basic research and material science under the perspective of spin-based electronic devices. One particular aspect, which we want to address in this contribution, is the generation of spin-polarized carriers in semiconductor quantum structures. This aspect is specific for the semiconductor material and can be considered without technological problems such as spin injection, inherent with the paradigmatic spin transistor proposed by Datta and Das.[1] Recently it has been demonstrated that in quantum well structures based on III-V compounds, a directed current inseparably linked to spin-polarized carriers and spin-split electronic states can be created by circularly polarized light employing nonlinear optical properties.[2,3] This effect belongs to the class of photogalvanic effects known for bulk semiconductors.[4]

The nonlinear optical response of matter under excitation by light with frequencies ω_1 and ω_2 is described in lowest order by a third rank tensor. The response is at the sum or difference frequency $\Omega = \omega_1 \pm \omega_2$. Special cases, with light from one intense light source ($\omega = \omega_1 = \omega_2$), are second harmonic generation ($\Omega = 2\omega$) and the photogalvanic effect ($\Omega = 0$). The latter is the generation of a directed current (double index summation understood)

$$j_\lambda = D_{\lambda\mu\nu} E_\mu(\omega) E_\nu(-\omega) \tag{1}$$

by applying light with the electric field $E_\mu(t) = E_\mu(\omega) e^{i\omega t}$ and $E_\mu^*(\omega) = E_\mu(-\omega)$. For j_λ to be real the third rank tensor $D_{\lambda\mu\nu}$ has to be symmetric with respect to complex conjugation together with interchange of μ and ν. Thus by decomposition of $D_{\lambda\mu\nu}$ into real and imaginary parts (being symmetric and antisymmetric, respectively, under interchange of the indices μ and ν) j_λ can be separated according to

$$j_\lambda = \chi_{\lambda\mu\nu}[E_\mu(\omega) E_\nu^*(\omega) + E_\mu^*(\omega) E_\nu(\omega)]/2$$

$$+ i\gamma_{\lambda\kappa}(\mathbf{E} \times \mathbf{E}^*)_\kappa, \tag{2}$$

where $\chi_{\lambda\mu\nu}$ is the real part of $D_{\lambda\mu\nu}$ and $\gamma_{\lambda\kappa}$ is a second-rank pseudo-tensor composed of the antisymmetric imaginary part of $D_{\lambda\mu\nu}$. The second term on the right-hand side of Eq. (2) can be expressed using $i(\mathbf{E} \times \mathbf{E}^*)_\kappa = \hat{e}_\kappa P_{\text{circ}} E_0^2$ with E_0 and $\hat{\mathbf{e}}$ being the electric field amplitude $|\mathbf{E}|$ and the unit vector pointing in the direction of light propagation, respectively. Because of the factor P_{circ}, indicating the degree of circular polarization, this term is identified with the circular photogalvanic effect (CPGE), while the first term of Eq. (2) contributes also for linearly polarized light and hence represents the linear photogalvanic effect (LPGE). Both effects require nonvanishing components of the tensor $D_{\lambda\mu\nu}$ which exist only in systems without a center of inversion, i.e., in bulk Si or Ge both effects are absent. However, it is important to note that both effects become possible due to symmetry reduction in QW structures based on these materials. This is demonstrated by the experiments presented below where the inversion symmetry was broken by preparation of compositionally stepped QW's and asymmetric doping of compositionally symmetric QW's.

II. EXPERIMENT

The measurements were carried out on *p*-type SiGe QW structures MBE grown on (001)- and (113)-oriented Si substrates. Two groups of (001)-grown asymmetric samples, whose potential profiles are sketched in Figs. 1(a) and 1(b), were fabricated in the following manner. One of the groups of samples was compositionally stepped [Fig. 1(a)] compris-
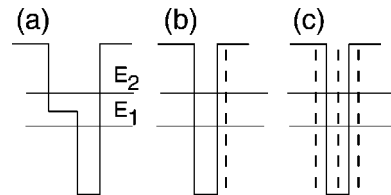
FIG. 1. Potentials profiles of investigated samples: (a) compositionally stepped QW, (b) asymmetrically doped compositionally symmetric QW, and (c) symmetric QW. The vertical dashed lines indicate the doping.
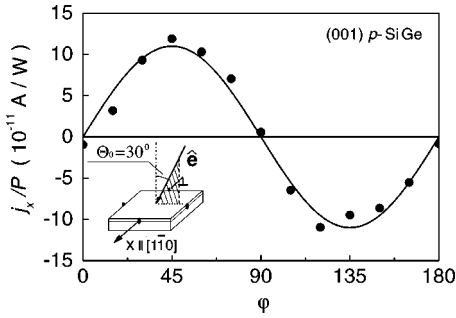
FIG. 2. Photogalvanic current j_x in (001)-grown and asymmetrically doped SiGe QW's normalized by the light power P and measured at room temperature as a function of the phase angle φ. The data were obtained under oblique incidence $\Theta_0 = 30°$ of irradiation at $\lambda = 10.6 \mu$m. The full line is fitted after Eq. (3). The inset shows the geometry of the experiment.

FIG. 3. Spectral dependence of CPGE (full dots) due to direct transitions between $hh1$ and $lh1$ valence subbands compared to the absorption spectrum obtained at 10 K. The absorption has been determined by transmission measurements making use a multiple-reflexion wave guide geometry shown in the inset. Results are plotted for (001)-grown and asymmetrically doped SiGe QW's.

ing ten QW's [Si$_{0.75}$Ge$_{0.25}$(4 nm)/Si$_{0.55}$ Ge$_{0.45}$(2.4 nm)] separated by 6 nm Si barriers. The second group of asymmetric structures had a single QW of Si$_{0.75}$Ge$_{0.25}$ composition which was doped with boron from one side only [Fig. 1(b)]. These structures are of the C_{2v} point group symmetry which has also been confirmed by the present experiment. Structures of the lower symmetry C_s were (113) grown with a Si/Si$_{0.75}$Ge$_{0.25}$(5 nm)/Si single QW one-side boron doped. As a reference sample a (001) grown compositionally symmetric and symmetrically boron doped multiple QW structure [Fig. 1(c)] of sixty Si$_{0.7}$Ge$_{0.3}$(3 nm) QW has been used. All these samples had free carrier densities of about 8 $\times 10^{11}$ cm^{-2} in each QW and were studied at room temperature. For (001)-oriented samples two pairs of Ohmic point contacts in the center of the sample edges with connecting lines along $x \| [1\bar{1}0]$ and $y \| [110]$ have been prepared (see inset in Fig. 2). Two additional pairs of contacts have been formed in the corners of the samples corresponding to the $\langle 100 \rangle$ directions. For (113)-oriented samples two pairs of contacts were centered along opposite sample edges pointing in the directions $x \| [1\bar{1}0]$ and $y \| [33\bar{2}]$ (see inset in Fig. 5).

A high power pulsed midinfrared (MIR) TEA-CO$_2$ laser and a far-infrared (FIR) NH$_3$ laser have been used as radiation sources delivering 100 ns pulses with radiation power P up to 100 kW. Several lines of the CO$_2$ laser between 9.2 and 10.6 μm and of the NH$_3$ laser[5] between $\lambda = 76$ and 280 μm have been used for excitation in the MIR and FIR range, respectively. The MIR radiation induces direct optical transitions between heavy hole and light hole subbands while the FIR radiation causes indirect optical transitions in the lowest heavy-hole subband. The laser light polarization was modified from linear to circular using a Fresnel rhombus and quartz $\lambda/4$ plates for MIR and FIR radiation, respectively. The helicity of the incident light was varied according to $P_{\text{circ}} = \sin 2\varphi$ where φ is the angle between the initial plane of linear polarization and the optical axis of the polarizer. For investigation of the LPGE linearly polarized radiation has been used. In this case α is the angle between the electric field vector and the x direction (see inset in Fig. 5). The current j generated by the polarized light in the unbiased

devices was measured via the voltage drop across a 50 Ω load resistor in a closed circuit configuration. The voltage was recorded with a storage oscilloscope. The measured current pulses of 100 ns duration reflect the corresponding laser pulses.

With illumination by MIR radiation of the CO$_2$ laser in (001)-oriented samples with asymmetric QW's a current signal proportional to the helicity P_{circ} is observed under oblique incidence indicating the CPGE (Fig. 2). We note that the samples were unbiased, thus the irradiated samples represent a current source. The current follows the temporal structure of the laser pulse intensity and changes sign if the circular polarization is switched from left to right handed. For $\langle 110 \rangle$ as well as for $\langle 100 \rangle$ crystallographic directions the photocurrent flows perpendicular to the wavevector of the incident light. The wavelength dependence of the photocurrent obtained between 9.2 and 10.6 μm corresponds to the spectral behavior of direct intersubband absorption between the lowest heavy hole and light hole subbands measured in transmission (see Fig. 3).

In the FIR range a more complicated dependence of the current as a function of helicity has been observed. In (001)-grown asymmetric QW's as well as in (113)-grown samples the observed dependence of the current on the phase angle φ may be described by the sum of two terms, one being $\propto \sin 2\varphi$ and the other $\propto \sin 2\varphi \cos 2\varphi$. In Fig. 4 experimental data and a fit to these functions are shown for a step bunched (113)-grown SiGe sample. The first term $\propto \sin 2\varphi$ is again caused by CPGE. The second term $\propto \sin 2\varphi \cos 2\varphi$ vanishes for circularly polarized radiation ($\varphi = 45° + m$ 90°, m is integer). This makes the assumption likely that this term is caused by the linear photogalvanic effect[2] with the electric field vector projected on the y direction. In order to prove that, the photocurrent has been investigated in response to a linearly polarized radiation. Indeed the LPGE could be observed with the current along both the x and the y direction. Figure 5 presents the measured dependence of j_x and j_y, as a function of the angle α between the plane of linear polarization and the axis x. The solid and the dashed curves in Fig. 5 show the fit after $j_x \propto \sin 2\alpha$ and $j_y \propto [\chi_+ - \chi_- \cos 2\alpha]$, respectively. Here χ_+ and χ_- are constants.

For both spectral ranges with (001)-grown samples a
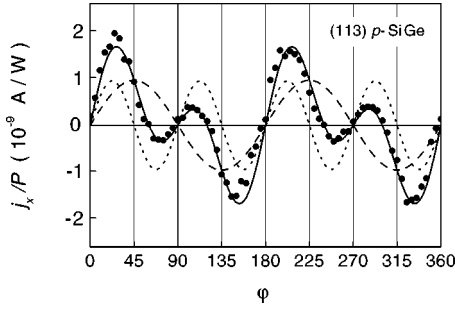
FIG. 4. Photogalvanic current in (113)-grown SiGe QW's normalized by the light power P as a function of the phase angle φ. The results were obtained under normal incidence of irradiation at $\lambda = 280\mu$m at room temperature. The full line is fitted after Eq. (6). Broken and dotted lines show $j_x \propto \sin 2\varphi$ and $j_x \propto \sin 2\varphi \cdot \cos 2\varphi$, respectively.

variation of the angle of incidence Θ_0 in the incidence plane around $\Theta_0 = 0$ changes the sign of the current. At normal incidence the current vanishes. This is observed for both the CPGE and the LPGE. For (113)-grown samples the current does not change its sign by the variation of Θ_0 and assumes its maximum at $\Theta_0 = 0$.

In symmetrically (001)-grown and symmetrically doped SiGe QW's no photogalvanic current has been observed in spite of the fact that these samples, in order to increase their sensitivity, contain substantially more QW's than the asymmetric structure described above.

III. PHENOMENOLOGICAL DESCRIPTION

Several point groups are relevant in connection with the photogalvanic experiments using (001)- and (113)-oriented $Si/Si_{1-x}Ge_x$ QW structures on which we report here. We consider structures with ideal abrupt interfaces. The point symmetry of a single (001)-oriented heterointerface between semiconductors with a diamond lattice is C_{2v} (the same as for zinc blende heterointerfaces). The symmetry of (001)-grown $Si/(Si_{1-x}Ge_x)_n/Si$ QW's depends on the number n of atomic layers forming the well. It is D_{2h} for even n and D_{2d} for odd n. In contrast to D_{2d} the point group D_{2h} has a center of inversion and thus forbids the second order response including both LPGE and CPGE as well as second-harmonic generation. An electric field (external or built-in) along the growth direction reduces the symmetry from D_{2h} or D_{2d} to C_{2v}. The point group C_{2v} includes the twofold rotation axis $C_2 \| [001]$ and the mirror planes $\sigma_{(110)}, \sigma_{(1\bar{1}0)}$. In real (001)-grown QW's with monoatomic height fluctuations such as steps, islands, and terraces, the local C_{2v} symmetry increases to C_{4v} upon averaging over a certain in-plane area (see Ref. 6). For symmetrical QW's with built-in electric fields or asymmetrical QW's (due to doping or different profiles of the left and right interfaces) the macroscopic symmetry is C_{2v} as for a single heterojunction. It should be noted here, that second harmonic generation has been detected in (001)-grown Si/SiGe QW's.[7] If an interface is grown along the low-symmetry axis $z \| [hhl]$ with $[hhl] \neq [001]$ or [111], the point group becomes C_s (see, e.g., Ref. 8) and contains only
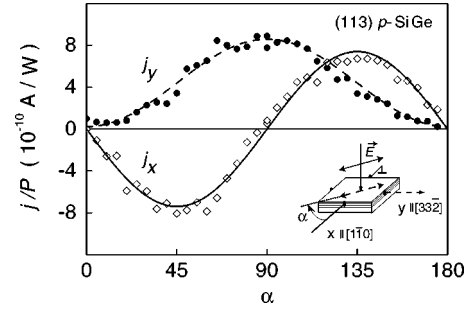
FIG. 5. Photocurrent j in response to linear polarized radiation for x and y directions as a function of the angle α between the plane of linear polarization and the axis x. The results were obtained in (113)-grown SiGe QW's under normal incidence of irradiation at $\lambda = 280\mu$m at room temperature. The broken line and the full line are fitted after Eq. (5).

two elements, the identity and one mirror reflection plane $\sigma_{(1\bar{1}0)}$. Asymmetric (hhl)-grown QW's retain the point-group symmetry C_s and thus allow CPGE and LPGE as is the case for zinc blende–based QW's grown on (113)-oriented substrates. The samples used in our experiments (see previous section) have C_{2v} or C_s symmetry for (001)- or (113)-grown structures, respectively.

CPGE and LPGE depend in a characteristic way on the angular configuration of the experimental setup (see previous section). One angle (φ) is used to describe the changing polarization of the incident light between linear $(\varphi = 0, 90°, 180°, \dots)$ and circular $(\varphi = 45°, 135°, \dots)$, the second (α) describes (for linear polarization) the angle between the plane of linear polarization and the x axis. Making use of the sample symmetry we derive these characteristic angular dependencies of the photocurrent j_λ of Eq. (2) on φ and α. In doing so we identify the coordinates x, y, z with the directions $[1\bar{1}0]$, $[ll(\bar{2}h)]$ and $[hhl]$, respectively, where $[hhl]$ ([001] or [113] in our case) is the growth axis of the QW structure. Due to carrier confinement in z direction the photocurrent in QW's has nonvanishing components only in x and y. Then, in a system of C_{2v} symmetry, the tensor $\boldsymbol{\gamma}$ describing the CPGE is characterized by two linearly independent components γ_{xy} and γ_{yx} and the second term of Eq. (2) reduces to

$$j_x = \gamma_{xy}\hat{e}_y P_{\text{circ}}E_0^2, \quad j_y = \gamma_{yx}\hat{e}_x P_{\text{circ}}E_0^2 \quad (3)$$

with $P_{\text{circ}} = \sin 2\varphi$. A photocurrent can be induced in this case only under oblique incidence (as in Fig. 2) because for normal incidence, $\hat{\mathbf{e}} \| [001]$ and hence $\hat{e}_x = \hat{e}_y = 0$.

The C_s symmetry allows CPGE and LPGE for normal incidence $\hat{\mathbf{e}} \| [hhl]$ because in this case the tensors $\boldsymbol{\gamma}$ and $\boldsymbol{\chi}$ have the additional nonzero components γ_{xz}, $\chi_{xxy} = \chi_{xyx}$, χ_{yxx}, and χ_{yyy}. As a result, under normal incidence, one has

$$j_x = \gamma_{xz}P_{\text{circ}}E_0^2 + \chi_{xxy}(E_x E_y^* + E_y E_x^*),$$

$$j_y = \chi_{yxx}|E_x|^2 + \chi_{yyy}|E_y|^2, \quad (4)$$

where $E_0^2 = |E_x|^2 + |E_y|^2$. In particular, for linearly polarized light

$$j_x = E_0^2 \chi_{xxy} \sin 2\alpha, \quad j_y = E_0^2 (\chi_+ + \chi_- \cos 2\alpha), \quad (5)$$

where $\chi_\pm = (\chi_{yxx} \pm \chi_{yyy})/2$. In the experimental setup, where the laser light is linearly polarized along x and a $\lambda/4$ plate is placed between the laser and the sample, Eqs. (4) reduce to

$$j_x = E_0^2 (\gamma_{xz} + \chi_{xxy} \cos 2\varphi) \sin 2\varphi,$$
$$j_y = E_0^2 (\chi_+ + \chi_- \cos 2\varphi). \quad (6)$$

The dependencies of Eqs. (3), (5), and (6) agree well with the experimental results for different SiGe QW's as shown in Figs. 2, 4, and 5. The tensors $\boldsymbol{\gamma}$ and $\boldsymbol{\chi}$ describe different physical mechanisms and, therefore, may depend differently on the excitation wavelength, material parameters, and temperature. In the present samples, for MIR excitation, the contribution of $\boldsymbol{\gamma}$ to the photocurrent is larger than that of $\boldsymbol{\chi}$ (Fig. 2) whereas for FIR excitation both effects CPGE and LPGE are of the same order of magnitude. This difference may be caused by the different optical excitation mechanisms: for MIR excitation direct transitions between subsequent subbands dominate while in the FIR only free carrier absorption within a subband is possible.

IV. MICROSCOPIC THEORY

The principal microscopic origin of a photon helicity driven current is the removal of spin degeneracy in the subband states due to the reduced symmetry of the quantum well structure.[3,9] For systems consisting of material components, which have inversion symmetry (here Si and Ge with diamond structure) and, as a consequence, only spin degenerate electron states, it has to be shown that spin degeneracy can be removed due to the symmetry (C_{2v} or C_s) of the investigated SiGe structures. It is caused by the appearance of **k**-linear terms in the Hamiltonian

$$H^{(1)} = \beta_{lm} \sigma_l k_m, \quad (7)$$

where **k** is the wave vector, the real coefficients β_{lm} form a pseudotensor (subjected to the same symmetry restrictions as $\boldsymbol{\gamma}$) and the σ_l are the Pauli spin matrices. In this section several scenarios will be presented which could contribute to β_{lm} in SiGe QW's with symmetries C_{2v} or C_s. As discussed in Ref. 3 the coupling between the carrier spin (σ_l) and wave vector (k_m) together with the spin-controlled dipole selection rules yields a net current under circularly polarized excitation. Depending on the photon energy this spin photocurrent can be either due to direct or indirect intersubband transitions. The former (latter) is realized in our experiments presented in Fig. 2 (Fig. 4).

Spin degeneracy results from the simultaneous presence of time reversal and spatial inversion symmetry. If one of these symmetries is broken the spin degeneracy is lifted. In our SiGe QW systems the spatial inversion symmetry is broken (the point groups C_{2v} and C_s do not contain the inversion operation) and, as a consequence, spin-dependent and **k**-linear terms appearing in the electron Hamiltonian lead to a splitting of the electronic subbands at finite in-plane wave

vector. Microscopically different mechanisms can lead to **k**-linear terms, which will be discussed here briefly.

A. Electric-field induced Rashba-like terms

In the context of spin related phenomena in QW structures most frequently the so-called Rashba term[10] is addressed, which is a prototype spin-orbit coupling term. It has axial symmetry and can exist as well in systems invariant under C_{2v} and C_s. Within the **k**·**p** theory the Rashba term can be understood as resulting from the couplings between conduction and valence band states mediated by the momentum operator (**k**·**p** coupling) and the space coordinate z in the electric confinement potential $V = eFz$ (F being the electric field). The matrix element of the latter can be expressed by the momentum matrix element p_{cv} divided by the gap energy E_g. It can be shown that, for the light holes in the basis $|lh1,1/2\rangle, |lh1,-1/2\rangle$ (as for the corresponding conduction electron states), the 2×2 Hamiltonian linear in **k** is given by

$$\beta_F \begin{bmatrix} 0 & -k_y - ik_x \\ -k_y + ik_x & 0 \end{bmatrix} = -\beta_F (\sigma_x k_y - \sigma_y k_x), \quad (8)$$

with

$$\beta_F = \frac{1}{3} eF \left(\frac{|p_{cv}|\hbar}{m_0 E_g} \right)^2. \quad (9)$$

The expression (8) is invariant under $C_{\infty v}$. The Rashba-like terms for heavy- and light-hole subband states have been discussed in Ref. 11.

B. Linear-k terms due to heavy-light hole mixing

The tetrahedral orientation of the chemical bonds, sticking out from an atom at the (001) interface to pairs of different atoms on either side, reduce the microscopic symmetry and give rise to a mixing of heavy- and light-hole states even at zero in-plane wave vector.[12] This mechanism, originally considered for interfaces between zinc blende compound semiconductors, exists as well for the SiGe interface. It can be considered in the envelope-function approach in the form of a δ-functional coupling Hamiltonian

$$H_{l\text{-}h} = \frac{\hbar^2}{m_0 a_0 \sqrt{3}} t_{l\text{-}h} \{\hat{J}_1, \hat{J}_2\} \delta(z - z_{if}), \quad (10)$$

where $\{\hat{J}_1, \hat{J}_2\} = (\hat{J}_1 \hat{J}_2 + \hat{J}_2 \hat{J}_1)/2$ is the symmetrized product of 4×4 matrices of the angular momentum components in the basis of the $J = 3/2$ states. In the given form (a_0 being the lattice constant and m_0 the mass of the free electron) $t_{l\text{-}h}$ is a dimensionless coupling parameter and z_{if} the position of the interface along the growth axis. For a $Si/(Si_{1-x}Ge_x)_n/Si$ QW with odd n the coefficients $t_{l\text{-}h}^{(L)}$ and $t_{l\text{-}h}^{(R)}$ at the left and right interfaces differ in sign as they do in zinc blende–based QW's.[12] However, in diamond-based structures interfaces can be shifted not only by an integer number of mono*molecular* layers (as in case of binary zinc blende systems) but by any number of mono*atomic* layers. A shift of the interface

by one monoatomic layer interchanges the role of axes $[1\bar{1}0]$ and $[110]$ and results in sign reversal of t_{l-h}. Thus the general relation

$$t_{l-h}^{(L)} = (-1)^{n+1} t_{l-h}^{(R)} \qquad (11)$$

is valid. The mixing due to H_{l-h} leads to a wave function at the bottom of the lowest heavy-hole ($hh1$) subband, which has the form

$$\varphi_{\pm 3/2}^{(hh1)} = C(z)|\Gamma_8, \pm 3/2\rangle \pm iS(z)|\Gamma_8, \mp 1/2\rangle, \qquad (12)$$

where $C(z), S(z)$ are real functions. In SiGe QW's with odd n $C(z)$ is even and $S(z)$ is odd with respect to reflection in the central plane of the QW layer (see for details Ref. 12). Now we take the contribution

$$\frac{\sqrt{3}\hbar^2\gamma_3}{m_0}\begin{bmatrix} 0 & k_z k_- & 0 & 0 \\ k_z k_+ & 0 & 0 & 0 \\ 0 & 0 & 0 & -k_z k_- \\ 0 & 0 & -k_z k_+ & 0 \end{bmatrix} \qquad (13)$$

to the bulk Luttinger Hamiltonian proportional to $k_z k_{\pm}$ ($k_{\pm} = k_x \pm i k_y$), consider it as a perturbation and calculate its matrix elements between the states of Eq. (12). The result presented in the form of a 2×2 matrix reads

$$H_{hh1}^{(1)} = \frac{2\sqrt{3}\hbar^2\gamma_3}{m_0} Q\begin{bmatrix} 0 & k_- \\ k_+ & 0 \end{bmatrix}, \quad Q = \int S(z)\frac{d}{dz}C(z)dz. \qquad (14)$$

In the same way one can derive **k**-linear terms for higher heavy-hole subbands as well as for light-hole subbands. In the latter case the **k**-linear Hamiltonian is proportional to the matrix

$$\begin{bmatrix} 0 & k_+ \\ k_- & 0 \end{bmatrix} = \sigma_x k_x - \sigma_y k_y.$$

We would like to emphasize that terms of this structure have been discussed so far only for material systems with bulk inversion asymmetry (BIA).[16] Note, that for QW's with even n the envelope functions $C(z), S(z)$ in Eq. (12) are of the same parity and the integral Q vanishes in agreement with the symmetry considerations.

C. k-linear terms in asymmetrical (hhl)-grown QW's

Invoking the theory of invariants,[13] the Hamiltonian acting in the twofold space of particles with spin 1/2 can be represented in terms of four independent 2×2 matrices (the unit matrix and the Pauli spin matrices). In addition to the Rashba term (which has this form) there could be similar expressions but with higher powers of the wave vector (or the electric field). The 4×4 Hamiltonian for holes, usually described in the basis of angular momentum eigenstates with $J = 3/2$, $M = \pm 3/2$, $\pm 1/2$, requires for its most general form 16 independent matrices formed from angular momentum matrices J_x, J_y, J_z, their powers and products. Thus in combination with tensor operators, composed of components of the momentum (or wave vector) and the electric field, new

terms are possible under C_{2v} and C_s. Some of these, which can be regarded as generalized Rashba terms, give rise to **k**-linear contributions in the hole subbands.

For asymmetrical (hhl)-grown QW's the relevant terms are odd in k_x and $\hat{J}_z$, e.g., for hole states those proportional to $\hat{J}_z k_x, \hat{J}_z k_x^3, \hat{J}_z k_x k_y^2, \hat{J}_z^3 k_x$, where $\hat{J}_z$ is the z component of the angular momentum operator in the coordinate system $x\|[\bar{1}10]$, $y\|[ll(\overline{2h})]$, $z\|[hhl]$. These terms result in hole subband dispersions of the form

$$E_{\nu j\mathbf{k}} = E_{\nu\mathbf{k}}^0 \pm \beta_\nu k_x, \qquad (15)$$

where $E_{\nu\mathbf{k}}^0$ is the hole subband dispersion calculated without **k**-linear terms.

The 4×4-Luttinger Hamiltonian, describing the valence band dispersion of bulk Si or Ge close to the center of the Brillouin zone

$$H_{\Gamma_8}(\mathbf{k}) = H_{\Gamma_8}^{(0)}(\mathbf{k}) - \frac{\hbar^2}{m_0}(\gamma_3 - \gamma_2)\hat{U}(\mathbf{k}),$$

can be split into a spherically symmetric part

$$H_{\Gamma_8}^{(0)}(\mathbf{k}) = \frac{\hbar^2}{2m_0}\left[\left(\gamma_1 + \frac{5}{2}\gamma_2\right)1_{4x4} - 2\gamma_2(\hat{\mathbf{J}}\cdot\mathbf{k})^2\right]$$

(1_{4x4} is the 4×4 unit matrix) and an anisotropic term with

$$\hat{U}(\mathbf{k}) = \sum_{\alpha\neq\beta}\{\hat{J}_\alpha, \hat{J}_\beta\}k_\alpha k_\beta.$$

The eigenvalues of the former are isotropic in **k**, while the latter term causes warping. In the coordinate system x, y, z and for $\mathbf{k} = (0, 0, k_z)$ this term can be written as (see Ref. 14)

$$\hat{U}'(k_z) = \frac{1}{2}\left\{(1 + 3\cos 2\theta)\left[\hat{J}_z^2 - \frac{1}{2}(\hat{J}_x^2 + \hat{J}_y^2)\right] - (1 - 3\cos^2\theta)\right.$$

$$\times (\hat{J}_x^2 - \hat{J}_y^2)\right\}\sin^2\theta k_z^2 + \sin\theta\cos\theta(3\cos^2\theta - 1)$$

$$\times\{\hat{J}_y, \hat{J}_z\}k_z^2, \qquad (16)$$

where θ is the angle between the axes $[hhl]$ and $[001]$. We may now treat the subband problem by considering $H_{\Gamma_8}^{(0)}(\mathbf{k}\|z)$ as leading term to calculate the subband energies at zero in-plane **k** and consider

$$\hat{V} = -\frac{\hbar^2}{m_0}\{2\gamma_2[\{\hat{J}_x, \hat{J}_z\}k_x + \{\hat{J}_y, \hat{J}_z\}k_y]k_z$$

$$+ (\gamma_3 - \gamma_2)\sin\theta\cos\theta(3\cos^2\theta - 1)\{\hat{J}_y, \hat{J}_z\}k_z^2\}$$

as a perturbation. Both terms of $\hat{V}$ cause a coupling between heavy ($M = \pm 3/2$)- and light ($M = \pm 1/2$)-hole states. The first term, representing the contributions of $H_{\Gamma_8}^{(0)}(\mathbf{k})$ proportional to $k_\pm k_z$, gives rise to this coupling for finite in-plane **k**, while the second, taken from the warping term, describes heavy-light hole coupling even for zero in-plane **k** (note that under C_s the angular momentum M ceases to be a good

quantum number). Treating $\hat{\mathcal{V}}$ in second order perturbation theory the cross terms between these two *l-h* coupling mechanisms yield **k**-linear contributions $\pm \beta k_x$ to the hole subband dispersion with

$$\beta = 2\sqrt{3} \frac{\gamma_2(\gamma_3 - \gamma_2)}{E_{lh1}^{(0)} - E_{hh1}^{(0)}} \left(\frac{\hbar^2}{m_0}\right)^2 S_1 S_2$$

and

$$S_1 = \int F_{hh1}(z) \frac{d}{dz} F_{lh1}(z) dz, \quad S_2 = \int F_{hh1}(z) \frac{d^2}{dz^2} F_{lh1}(z) dz.$$

Note that in symmetric QW's the subband envelope functions $F_{hh1}(z)$ and $F_{lh1}(z)$ are even. Thus, S_1 and the splitting would vanish in this case in accordance with the general symmetry considerations.

D. Electric-field-induced terms proportional to $\hat{J}_z k_x$

As mentioned above we may consider also invariants constructed with the angular momentum matrices in the basis $J = 3/2$ and tensor components combining k_α and electric field F_α ($\alpha = 1,2,3$):

$$H^{(1)} = d_1 [\hat{V}_1(F_2 k_3 + F_3 k_2) + \hat{V}_2(F_3 k_1 + F_1 k_3)$$
$$+ \hat{V}_3(F_1 k_2 + F_2 k_1)] \tag{17}$$

and

$$H^{(3)} = d_3 [\hat{J}_1(F_2 \kappa_3 + F_3 \kappa_2) + \hat{J}_2(F_3 \kappa_1 + F_1 \kappa_3)$$
$$+ \hat{J}_3(F_1 \kappa_2 + F_2 \kappa_1)], \tag{18}$$

with $\hat{V}_1 = \{\hat{J}_1, \hat{J}_2^2 - \hat{J}_3^2\}$ and $\kappa_1 = k_1(k_2^2 - k_3^2)$ (and cyclic permutations of these expressions). Transforming to the coordinate system x,y,z as before these terms provide a first-order perturbation correction to subband states $|\nu s \mathbf{k}\rangle$ [calculated without odd-$\mathbf{k}$ terms and symmetric with respect to the mirror reflection in the plane (hhl) as defined in Ref. 15]. The weighting factor for the spin-splitting term in the subband ν reads

$$\beta_\nu = \sin\theta\cos\theta(1 - 3\cos^2\theta)F_z \left(-\frac{d_1}{2}\langle \nu s \mathbf{k}|\hat{J}_z^3|\nu s \mathbf{k}\rangle \right.$$

$$\left. + d_3 \langle \nu s \mathbf{k}|\hat{J}_z \hat{k}_z^2|\nu s \mathbf{k}\rangle \right), \tag{19}$$

with θ as defined before and $\hat{k}_z^2 = -\partial_z^2$. The procedure used to obtain β_ν, Eq. (19), is similar to that of Ref. 16 when deriving terms linear in the in-plane momentum of a QW from cubic terms of the bulk band structure. Note that, as compared with d_1, the coefficient d_3 is not relativistically small and contributions from the second term in Eq. (19) can be of the same order as (or even exceed) the first term.

The four scenarios presented in this section demonstrate the possibility of **k**-linear spin-splitting terms in the subband dispersion of SiGe QW's due to the low (C_{2v} or C_s) symmetry of these structures. Of these only scenario *A* has been discussed before[11] for GaAs based structures, while the others (*B*, *C*, and *D*) are new. Their relative importance for the observed photocurrents, depending on the material parameters and on the geometry and composition of the individual QW structure, could be evaluated only by a calculation of the tensors χ and γ. Such calculations are far beyond the scope of the present investigation.

V. CONCLUSIONS

In our experiments, carried out for different *p*-type QW structures based on the SiGe material system we have demonstrated the possibility to create a photon helicity driven stationary current due to the circular photogalvanic effect. Our experiments show the characteristic angular dependencies derived from the phenomenological formulation of the linear and circular photogalvanic effects. The experiments have been performed in different regimes of photon energies allowing for direct and indirect intersubband transitions. The experimental results prove the removal of spin degeneracy of hole subbands in asymmetric SiGe QW's. We analyze the symmetry of the QW's under investigation and present different scenarios that can lead to spin-dependent **k**-linear terms in the hole subband Hamiltonian, which are prerequisite for the appearance of the observed photocurrent. Our results provide the important information that spin-related phenomena, which so far have been considered to be specific for QW structures based on zinc blende materials, exist also in the SiGe QW systems. In particular spin sensitive bleaching of absorption at direct intersubband transitions may be recorded by the saturation of LPGE and CPGE at high power levels allowing to conclude on spin relaxation times as most recently demonstrated with GaAs QW's.[17]

[1] S. Datta and B. Das, Appl. Phys. Lett. **56**, 665 (1990).

[2] S.D. Ganichev, H. Ketterl, W. Prettl, E.L. Ivchenko, and L.E. Vorobjev, Appl. Phys. Lett. **77**, 3146 (2000).

[3] S.D. Ganichev, E.L. Ivchenko, S.N. Danilov, J. Eroms, W. Wegscheider, D. Weiss, and W. Prettl, Phys. Rev. Lett. **86**, 4358 (2001).

[4] E.L. Ivchenko and G.E. Pikus, *Superlattices and Other Heterostructures. Symmetry and Optical Phenomena*, Vol. 110 of

Springer Series in Solid State Sciences (Springer-Verlag, Berlin, 1995).

[5] S.D. Ganichev, Physica B **273-274**, 737 (1999).

[6] D.J. Bottomley, H.M. Van Driel, and J.-M. Baribeau, *Proceedings of the 22nd ICPS* (World Scientific, Singapore, 1994), p. 1572.

[7] M. Seto, M. Helm, Z. Moussa, P. Boucaud, F.H. Julien, J.M. Lourtioz, J.F. Nützel, and G. Abstreiter, Appl. Phys. Lett. **65**, 2969 (1994).

[8] D.J. Bottomley, H. Omi, and T. Ogino, J. Cryst. Growth **225**, 16 (2001).

[9] S.D. Ganichev, E. L. Ivchenko, and W. Prettl, Physica E (Amsterdam) **14**, 166 (2002).

[10] Yu.A. Bychkov and E.I. Rashba, J. Phys. C **17**, 6039 (1984).

[11] R. Winkler, Phys. Rev. B **62**, 4245 (2000).

[12] E.L. Ivchenko, A.Yu. Kaminski, and U. Rössler, Phys. Rev. B **54**, 5852 (1996).

[13] G.L. Bir and G.E. Pikus, *Symmetry and Strain-induced Effects in Semiconductors* (Wiley, New York, 1974).

[14] M.V. Belousov, E.L. Ivchenko, and A.I. Nesvizhskii, Phys. Solid State **37**, 763 (1995).

[15] I.A. Merkulov, V.I. Perel, and M.E. Portnoi, Sov. Phys. JETP **72**, 669 (1991).

[16] M.I. D'yakonov and V.Yu. Kachorovskii, Sov. Phys. Semicond. **20**, 110 (1985).

[17] S.D. Ganichev, S.N. Danilov, V.V. Bel'kov, E.L. Ivchenko, M. Bichler, W. Wegscheider, D. Weiss, and W. Prettl, Phys. Rev. Lett. **88**, 057401 (2002).